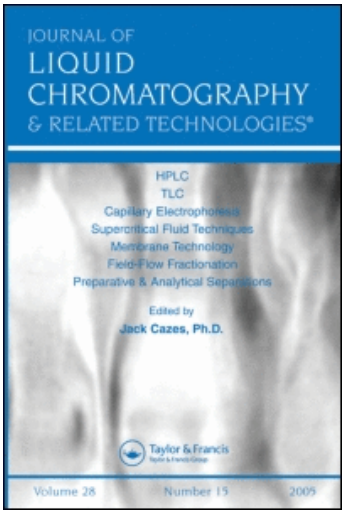

Journal of Liquid Chromatography & Related Technologies

Publication details, including instructions for authors and subscription information:
http://www.informaworld.com/smpp/title~content=t713597273

Modeling, Simulation, and Experimental Evaluation of Continuous Chromatographic Separation of Ketamine Enantiomers on MCTA

Amaro Gomes Barreto Jr.[a]; Ivanildo José da Silva Jr.[b]; Marco Antônio Garcia dos Santos[c]; Vinicius de Veredas[c]; Cesar Costapinto Santana[c]

[a] Departameto de Engenharia Quimica, Escola de Quimica da Universidade Federal do Rio de Janeiro, Edificio do Centro de Technologia, Rio de Janeiro, RJ, Brasil [b] Grupo de Pesquisa em Separacoes por Adsorcao-GPSA, Departamento de Engenharia Quimica, Centro de Tecnologia, Universidade Federo do Cerara, Campos do Pici, Fortaleza, CE, Brasil [c] Universidade Estadual de Campinas-UNICAMP, Faculdade de Engenharia Química, Departamento de Processos Biotecnológicos, Campinas, SP, Brasil

To cite this Article Barreto Jr., Amaro Gomes , Silva Jr., Ivanildo José da , dos Santos, Marco Antônio Garcia , Veredas, Vinicius de and Santana, Cesar Costapinto(2008) 'Modeling, Simulation, and Experimental Evaluation of Continuous Chromatographic Separation of Ketamine Enantiomers on MCTA', Journal of Liquid Chromatography & Related Technologies, 31: 20, 3057 — 3076

To link to this Article: DOI: 10.1080/10236660802479507

URL: http://dx.doi.org/10.1080/10236660802479507

Journal of Liquid Chromatography & Related Technologies®, 31: 3057–3076, 2008

ISSN: 1082-6076 print/1520-572X online
DOI: 10.1080/10236660802479507

Modeling, Simulation, and Experimental Evaluation of Continuous Chromatographic Separation of Ketamine Enantiomers on MCTA

Amaro Gomes Barreto Jr.,[1] Ivanildo José da Silva Jr.,[2] Marco Antônio Garcia dos Santos,[3] Vinicius de Veredas,[3] and Cesar Costapinto Santana[3]

[1]Departameto de Engenharia Quimica, Escola de Quimica da Universidade Federal do Rio de Janeiro, Edificio do Centro de Technologia, Rio de Janeiro, RJ, Brasil
[2]Grupo de Pesquisa em Separacoes por Adsorcao-GPSA, Departamento de Engenharia Quimica, Centro de Tecnologia, Universidade Federo do Cerara, Campos do Pici, Fortaleza, CE, Brasil
[3]Universidade Estadual de Campinas-UNICAMP, Faculdade de Engenharia Química, Departamento de Processos Biotecnológicos, Campinas, SP, Brasil

Abstract: Results on the chiral separation of ketamine enantiomers by simulated moving bed (SMB) chromatography using microcrystalline cellulose triacetate (MCTA) columns are reported. Experimental data obtained with the SMB laboratory unit showed purities above 99.5% in the raffinate stream and above 97.7% in the extract stream. A simulation approach based on true moving bed (TMB) was applied to validate the performance of the SMB in steady state regime, taking into account the non-linear isotherms, non-ideal effects, and the non-homogeneities of the eight columns. The experimental and calculated results are in agreement with the internal profiles calculated by the TMB approach.

Keywords: Chiral separation, Equilibrium theory, Ketamine, Liquid chromatography, Simulated moving bed

Correspondence: Cesar Costapinto Santana, Universidade Estadual de Campinas – UNICAMP, Faculdade de Engenharia Química, Departamento de Processos Biotecnológicos. P.O. Box: 6066. CEP: 13083-970, Campinas-SP, Brazil. E-mail: santana@feq.unicamp.br

NOMENCLATURE

b	Isotherm parameter ($L \cdot g^{-1}$)
c	Liquid phase concentration ($g \cdot L^{-1}$)
D_L	Axial dispersion coefficient ($cm^2 \cdot min^{-1}$)
H	Henry constant
k_m	Overall mass transfer coefficient (min^{-1})
L	Column length (cm)
m	Dimensionless flow-rate
Pe	Dimensionless number
Q	Flow-rate ($mL \cdot min^{-1}$)
q	Solid phase concentration ($g \cdot L^{-1}$)
q^*	Solid phase average concentration ($g \cdot L^{-1}$)
q_m	Saturation capacity ($g \cdot L^{-1}$)
t	Time (min)
t^*	Switch time
u_s	Solid phase velocity ($cm\ min^{-1}$)
V	Column volume
z	Axial coordinate
	Greek symbols
α	Dimensionless number
γ	Dimensionless number
ε	Total porosity
ν_f	Liquid phase flow velocity ($cm \cdot min^{-1}$)
	Subscripts
X	Extract
E	Eluent
F	Feed
R	Raffinate
i	Component (i = 1,2)
j	Section

INTRODUCTION

Simulated moving-bed (SMB) technology has been applied since the 1960s by Universal Oil Products for large scale separations in the petrochemical industry. Nowadays, the application of SMB for preparative and production scale separation of fine chemical and pharmaceutical products, and in particular enantiomers, is gaining increasing importance.[1,2] Moreover, chiral stationary phases show generally low or moderate values in the separation factors (between 1.1 and 1.4), and this results in more severe requirements for the performance of the SMB than for the other previous industrial separation process. However, compared to the batch process, SMB applications are hindered by a much higher degree of process complexity. Hence, for the successful development of new applications in the pharmaceutical industry, a more comprehensive understanding of the SMB process is required.[3]

SMB is a continuous apparatus, whose principle of operation can be best described with reference to equivalent true moving bed (TMB). In a TMB (Figure 1a), the liquid and solid phase flows are carried out in opposite directions. The inlet (feed and desorbent) and outlet (extract and raffinate) ports are fixed along the unit. According to the position

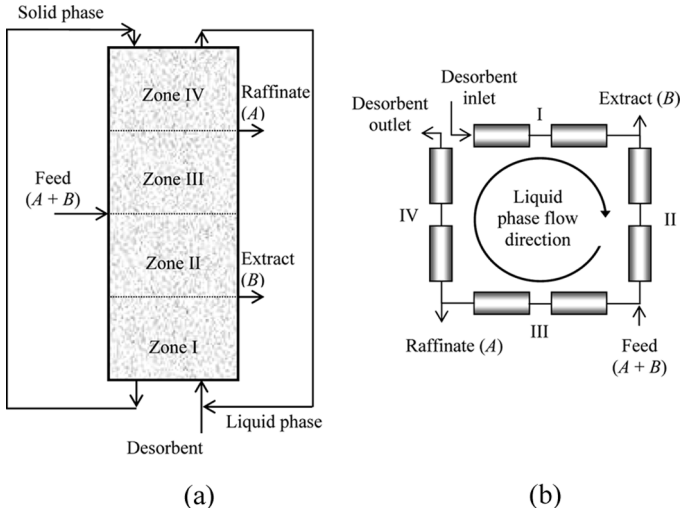

Figure 1. Counter-current unit scheme for continuous adsorptive separations of binary mixtures (*A*–weakly adsorbed component; *B*–strongly adsorbed component): (a) true moving-bed with four zones; (b) opened loop simulated moving-bed with four zones (two columns per zone).

of the inlet and outlet streams, four different operational sections can be distinguished: section I located between the eluent and extract streams, section II located between the extract and feed streams, section III located between the feed and raffinate streams, and section IV located between the raffinate and desorbent streams. The net flow rate has to be selected in each section in order to ensure the regeneration of adsorbent in section I, the desorption of the less strongly adsorbed component in section II, the adsorption of the more strongly adsorbed component in section III, and the regeneration of the desorbent in section IV. These conditions will guarantee the success of the separation, as the more retained component moves to the extract port with the solid phase and the less retained component moves to the raffinate port with the liquid phase.[4–6]

The major problem in TMB operations associated to the movement of the solid phase was overcome by the introduction of SMB technology. An SMB opened loop unit (Figure 1b) consists of a set of interconnected columns in series with valves and tubing forming a circuit. This circuit is divided into four zones with two inlet ports (feed and desorbent) and three outlet ports (raffinate, where a low affinity solute *A* is removed, an extract, where a high affinity solute *B* is removed, and a pure desorbent). The inlet and outlet ports are periodically moved in the liquid flow direction by multiple position valves, causing an apparent countercurrent

movement between the liquid and the solid phase. Similar to batch chromatography, solute *A* migrates faster than solute *B* in the liquid flow direction. In a four zone SMB, solute *A* adsorption occurs in zone IV, while its desorption occurs in zone II. Solute *B* adsorption occurs in zone III, and solute A desorption occurs in zone I.[7]

SMB units exhibit important advantages, in comparison to batchwise preparative chromatography. In particular, these are due to the continuous nature of the operation and to an efficient use of the stationary and mobile phases, which allows the decrease of the mobile phase (desorbent) requirement and the improvement of the productivity per unit time and unit mass of the stationary phase. Moreover, high performances can be achieved even at rather low values of selectivity and with a relatively small number of theoretical plates. These features of SMB units are due to the fact that, contrary to preparative chromatography, the concentration profiles of the components to be separated are allowed to overlap along the adsorption beds, the requirement being that the components are pure only at the extract and raffinate outlet locations. Due to these positive features, SMB is particularly attractive in the case of enantiomer separation, since it is difficult to separate enantiomers by conventional techniques.[8]

Most of the reported results consider that all the columns have identical characteristics during experimental analyses, and optimizations of operating conditions were performed when average values were applied. Although the same batch of packing material may be used, it is very difficult to manufacture columns with the same characteristics.[9] The differences between columns arise from the practical impossibility of packing identical columns. The packing procedure causes local fluctuations of the packing density, which are highly irreproducible. Small relative variations of the local packing density, hence of the porosity, result in larger fluctuations of permeability, hence local mobile phase velocity. Because the distribution of these differences is not reproducible, column to column porosity and permeability variations are observed.[10] Recently, some authors analyzed SMB performance considering the nonhomogeneity due to the changes in porosities.[3,10–12] In all the cases, the different characteristics of the columns were represented through the values of measured porosities for each column, allowing operational condition analysis based on the application of mathematical models in the steady state (TMB approach) and dynamic state (SMB approach).

Ketamine (Figure 2) is commercially available as a racemate (*S*- and *R*-ketamine). It is a dissociate anesthetic agent that has been widely used in clinical practice.[13,14] *S*-ketamine is four times more potent in analgesia than *R*-ketamine.[13] In addition, it does not induce the undesirable psychological reactions, such as vivid dreams and hallucinations in human beings, as these collateral effects are attributed to *R*-ketamine.[15]

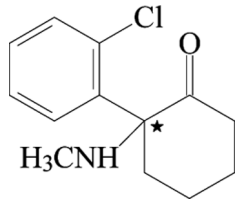

Figure 2. Chemical structure of ketamine. The symbol (★) denotes the chiral center.

Ketamine resolution has been reached in commercial applications by diastereomeric resolution,[16,17] which is one of the most traditional and still very popular techniques in the field of enantioseparation. The main disadvantage of this is the requirement for several reprocessing steps, increasing the overall processing time.[18]

Ketamine enantiomers were separated in our research group using a single column microcrystalline cellulose triacetate (MCTA) such as a chiral column.[19,20] These authors concluded that the resistance to mass transfer of ketamine enantiomers is very low in this chiral column, and that the adsorption isotherms presented a high saturation capacity. Silva et al. (2005),[20] also reported the effect of the temperature on the equilibrium and mass transfer in the chromatographic separation of ketamine on MCTA. An improvement in the resolution with an increase in the temperature due to more favorable kinetic of mass transfer was observed. A previous paper reported by Santos et al. (2004),[7] describes the continuous enantioseparation of ketamine in a semipreparative scale SMB unit, using MCTA as a chiral column providing a suitable separation of the two enantiomers with virtually 100% purification. A limitation, however, is the low productivity of the process in the laboratory unit, around 0.15 to 0.5 g/day.

A promising alternative to increase the productivity of *S*-ketamine purification is the coupling of fractional crystallization with an SMB unit.[21] These authors have shown that the ternary phase diagram of the S and R-ketamine in ethanol (solvent previously used by Santos et al. (2004))[7] present two eutectic points corresponding to the 75% enantiomeric excess of each species. This indicates that selective crystallization requires an enriched solution with a composition above the eutectic points.

In this study, the modeling, simulation and operation of SMB units to separate ketamine enantiomers were investigated. The modeling and simulation were carried out using the TMB mathematical approach, taking into account nonlinear isotherms, axial dispersion, and film resistance to mass transfer and heterogeneities of the packing columns. The

operational conditions were chosen for different feed concentration in order to obtain high purity of *S*-ketamine in the raffinate stream. The main contribution of this paper is to show that the TMB non-ideal mathematical model, taking into account non-homogenous columns, is capable of adequately representing the purities obtained experimentally, with the main focus being on those operating conditions whose experimental results are not adequately represented by an ideal model and non-homogenous columns.

MODELING OF AN SMB UNIT – TMB MODELING APPROACH

In general, the modeling of an SMB unit usually follows either one of the two basic approaches:[22]

1. The TMB approach. Countercurrent motion of a solid is actually taken into account and convenient equivalence relations are used to relate the results with an SMB unit.
2. The SMB approach. Each bed is analyzed individually and the periodic change in the boundary limit conditions is taken into account.

The TMB approach has the advantage of reducing the time analysis of the countercurrent sections. Concentration profiles build up around the feed node within the equipment and a single band profile is obtained at a steady state. On the other hand, the SMB approach examines each bed or subsection individually. At each switching time, the boundary conditions in all the columns must be updated and the steady state is not strictly reached. Instead, an axial motion of the band profiles occurs in a steady periodic fashion repeated at every period. TMB analysis has also the advantage of allowing the direct calculation of the steady state performance, by simply setting the time dependent terms in the model equations equal to zero and solving it.[22] SMB analysis has to calculate the transient response in order to reach the steady state solution, which may take a long time.

Due to their continuous countercurrent nature, after the start up, transient TMB units achieve a steady state, where every process variable remains constant in each location in the unit. On the contrary, the stationary regime of an SMB unit is a cyclic steady state, in which the unit exhibits the same time dependent behavior during each time period between two successive switches of the inlet and outlet ports. Therefore, even though a small difference will appear between these two strategies, the prediction of the performance of an SMB operation can be done using the TMB approach since the geometric and kinematic conversion rules given by Table 1 are fulfilled.[22,23]

Table 1. Equivalence relations between SMB and TMB units

	SMB	TMB
Solid phase:		
Velocity	0	$u_s = L/t^*$
Flow rate	0	$Q_S = u_s(1-\varepsilon)A$
Liquid phase:		
Velocity	u_k^{SMB}	$u_j^{\mathrm{TMB}} = u_k^{\mathrm{SMB}} - u_s^a$
Flow rate	Q_k^{SMB}	$Q_j^{\mathrm{TMB}} = Q_k^{\mathrm{SMB}} - \varepsilon V_c/t^{*a}$

[a]Equivalence for an SMB column k belonging to section j.

Mihlbachler et al. (2001) applied the equilibrium theory in order to obtain the flow rates through the four sections of an SMB process taking into account the characteristics of the different columns used. The liquid and solid flow ratio rates are given by:

$$\mathrm{r_j} = \frac{\mathrm{Q_j^{SMB} t^*}}{\mathrm{V}} \tag{1}$$

The separation region in non-linear conditions was defined by Mihlbachler et al. (2004),[12] using the Langmuir isotherm and taking into account the differences in the column porosities, according to Inequations (2) to (4), such as:

$$\mathrm{H_{2,j}^* < r_1} \tag{2}$$

$$\mathrm{r_{2,cr}(r_2, r_3) < r_2 < r_3 < r_{3,cr}(r_2, r_3)} \tag{3}$$

$$\begin{aligned} \mathrm{0 < r_4 < r_{4,cr}} = \varepsilon_\mathrm{j} + \frac{(1-\varepsilon_\mathrm{j})}{2}\Big[\mathrm{H_{1,j}^* + r_3 + b_1 c_1^f (r_3 - r_3).} \\ \mathrm{-\sqrt{[H_{1,j}^* + r_3 + b_1 c_1^f (r_3 - r_3)]^2 - 4 H_{1,j}^* r_3}}\Big] \end{aligned} \tag{4}$$

where, $\mathrm{H_{i,j}}^* = \mathrm{H_{i,j}}(1-\varepsilon_\mathrm{j}) + \varepsilon_\mathrm{j}$, $\mathrm{r_{2,cr}}$ and $\mathrm{r_{3,cr}}$ are obtained from Equation 1.

The mathematical non-ideal model used for the simulation of the steady state of equivalent TMB system takes into account the axial dispersion flow for the liquid phase, plug flow for the solid phase movement in the opposite direction to the fluid phase, linear driving force (LDF) for the intraparticle mass transfer rate, and adsorption equilibria described by the Langmuir isotherm. The system is approximated as a constant separation factor system, although in fact some variation of separation

factor with composition is observed.[24] In the model formulation, the following assumptions have been considered:

- Negligible thermal effects;
- Bed void fraction, radius and particle porosity are constant along the columns;
- Constant flow rate in each section;
- Negligible pressure gradient in the column.

According to these assumptions, the TMB dimensionless model can be written as follows:

Mass balance for specie i in a j zone volume element:

$$\frac{1}{Pe_j}\frac{d^2c_{i,j}}{dz^2} - \frac{dc_{i,j}}{dz} - \frac{1-\varepsilon_j}{\varepsilon_j}\frac{\alpha}{\gamma_j}(q^*_{i,j} - q_{i,j}) = 0 \tag{5}$$

The dimensionless numbers present in the model equations are

$$Pe_j = v_{f,j}L/D_{L,j}, \alpha = LK_m/u_s \quad \text{and} \quad \gamma_j = v_{f,j}/u_s.$$

Boundary conditions:

$$z = 0, \quad \left.\frac{dc_{i,j}}{dz}\right|_{z=0} = Pe_j(c_{i,j}|_{z=0} - c^f_{i,j}) \tag{6}$$

where, $c^f_{i,j}$ is the concentration of the i component, on the j section inlet, defined by:

$$c^f_{i,1} = \frac{Q_4 c_{i,1}(z=1)}{Q_1} \tag{7}$$

$$c^f_{i,j} = c_{i,j-1}(z=1), \quad \text{for } j = 2 \text{ and } 4 \tag{8}$$

$$c^f_{i,3} = \frac{Q_F c_{i,F} + Q_2 c_{i,2}(z=1)}{Q_3} \tag{9}$$

$$z = 1, \quad \left.\frac{dc_{i,j}}{dz}\right|_{z=1} = 0 \tag{11}$$

Mass balance to the solid phase for specie i:

$$\frac{dq_{i,j}}{dz} + \alpha_j(q^*_{i,j} - q_{i,j}) = 0 \tag{12}$$

Boundary conditions:

$$q_{i,j}\big|_{z=0} = q_{i,j-1}\big|_{z=1} \text{ and } q_{i,1}\big|_{z=0} = q_{i,4}\big|_{z=1} \tag{13}$$

Global mass balance at the nodes of the inlet and outlet streams are:
Eluent node:

$$Q_E = Q_1 \tag{14}$$

Extract node:

$$Q_2 = Q_1 - Q_X \tag{15}$$

Feed node:

$$Q_3 = Q_2 + Q_F \tag{16}$$

Raffinate node:

$$Q_4 = Q_3 - Q_R \tag{17}$$

In Equations (14) to (17), Q_j is the flow rate through section j, related with the interstitial velocity, defined by ν_j. Q_E is the desorbent flow rate, Q_X is the extract flow rate, Q_F is the feed flow rate and Q_R is the raffinate flow rate.

The adsorption isotherm is described by a Langmuir equation, represented by Equation (18).

$$q^*_{i,j} = f(c_{i,j}) = \frac{H_i c_{i,j}}{1 + \sum_{i=1}^{n=2} b_i c_{i,j}} \tag{18}$$

where, H_i and b_j are Henry and associate constants of the Langmuir isotherm of the ith component at section j, respectively.

The set of Equations (5) to (18) were numerically solved. The axial coordinate was discretized using finite volumes with appropriate quadratic upwind interpolation.[25,26] The set of the nonlinear algebraic equation was solved by NEQNF routine implemented in IMSL.[27]

EXPERIMENTAL

Chemicals and Reagents

The mobile phase used in this work was ethanol HPLC grade, J. T. Baker (USA), in which ketamine and 1,3,5, tri-*tert*-butylbenzene (TTBB) are

easily dissolved. Ketamine is supplied by the Cristália Company (Itapira-SP, Brazil). TTBB was purchased from Sigma-Aldrich (USA). MCTA presents broad applicability and low cost, when compared to other CSPs, and was purchased from the Macherey–Nagel Company (Germany). The adsorbent particles have 15–25 μm diameters. The stainless steel columns (20×0.77 cm ID) were packed with MCTA, using methanol as a solvent. Before packing, the swelling of MCTA was carried out through boiling it in ethanol for about 30 min. TTTB and ketamine were dissolved in ethanol. These solutions were previously degasified in a Cole Parmer 8892 ultrasonic bath.

SMB Unit

The open loop laboratory scale SMB unit was previously described by Santos et al. (2004)[7] The SMB configuration has eight stainless steel columns (20×0.77 cm I.D.) distributed in four zones (two columns per zone). The desorbent is recycled outside of the series of columns by using a multiposition valve instead of a solvent reflux pump. Another four multiposition valves are responsible for the position change of feed, desorbent inlet, raffinate, and extract at preset switch times. These valves are connected to four semipreparative liquid chromatographic pumps (Shimadzu model LC-6AD). A Shimadzu membrane degasser model DGU-14A was used to avoid air bubbles in the system. In Figure 3, some details of the complete setup are shown. Multiposition valves (Valco Instruments Co.) are electrically commanded and linked to a computer by a data acquisition board. Each valve automatically operates the unit at the selected flow rates by a program developed with the Labview software. The unit also contains a sampling valve connected to one of the columns of the series, which allows collection of internal samples. Analysis of these samples enables the determination of the internal concentration profiles of each enantiomer, which illustrates the dynamics of separation inside the series of columns.

The total amount of solute in raffinate and extract were determined by online monitoring with an UV/VIS detector (Shimadzu model SPD-10AV) equipped with a flow cell. The difference between these concentrations can be determined with a polarimetric detector (Jasco P-1010) also equipped with a flow cell. A similar procedure for the quantitative detection of chiral molecules was successfully used by Zenoni et al. (2000).[28]

In order to ensure the purity of the streams, offline monitoring was carried out. Samples were collected throughout the experimental run, for subsequent analysis in an HPLC system (equipped with Shimadzu detector model SPD-10AV and two Shimadzu model SPD-10AS pumps), which furnishes values of purity averaged throughout the collection time.

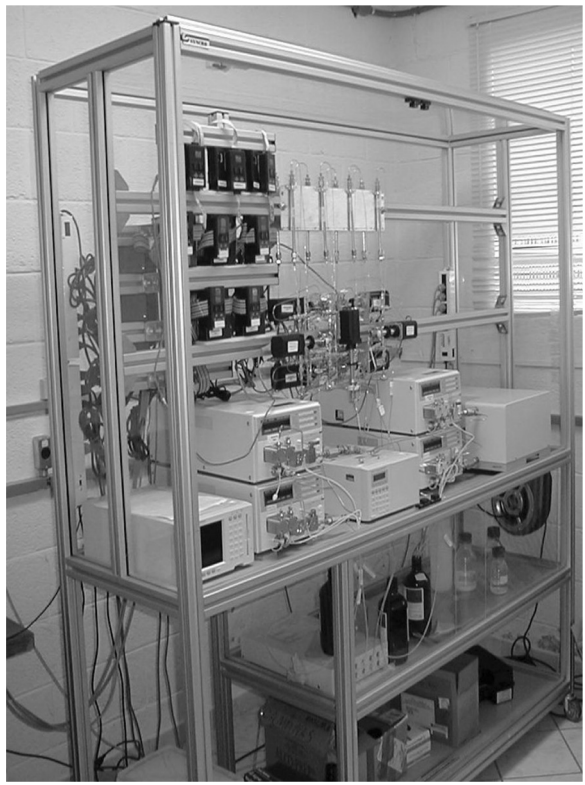

Figure 3. SMB unit with eight MCTA columns divided into four zones (2-2-2-2 configuration).

The column used for the HPLC tests was packed with the same stationary phase (MCTA) as that employed in the SMB columns (20×0.46 cm).

Column Characterization and Adsorption Isotherm Parameters

Batch experiments were performed in a HPLC system (equipped with a Waters UV detector model 2487, two Waters model 1525 pumps, and a digital data acquisition system) in order to obtain the column characteristics and adsorption isotherm data. Each column of the SMB system was characterized in terms of the porosities and Henry coefficients by pulse experiments with an inert tri-*tert*-butylbenzene compound (TTBB) and pure enanatiomers, as described by Santos et al. (2004).[7] The non-linear equilibrium data was previously reported by Silva et al. (2005).[19] The results are shown in Tables 2 and 3. The large value of selectivity factor (α) indicates easy separation.

Table 2. Column characteristic of an SMB unit

Column	t_0 (min)	ε_T	Retention time, t_R (min)		Henry coefficient, H		Selectivity (α)
			R	*S*	*R*	*S*	
1	6.00	0.64	21.60	12.87	4.71	2.07	2.3
2	5.99	0.64	22.39	13.41	4.93	2.23	2.2
3	6.16	0.66	23.73	14.36	5.57	2.60	2.1
4	6.53	0.70	23.41	14.22	6.07	2.76	2.2
5	6.39	0.69	23.91	15.75	5.99	3.20	1.9
6	6.26	0.67	23.57	15.98	5.67	3.18	1.8
7	6.41	0.69	24.04	15.53	6.08	3.15	1.9
8	6.42	0.68	23.46	15.00	5.89	2.97	2.0
Average	6.27	0.67	23.3	14.4	5.6	2.7	2.0

SMB Experimental Runs

Before experimental runs in SMB units, the operating conditions (liquid ratio and solid flow rates) were obtained based on the triangle theory for non-linear isotherms. The flow rates of extract and raffinate streams were monitored continuously by a flow meter during each cycle. Online monitoring of UV/Vis and polarimeter was carried out in order to observe the concentration behavior for each enantiomer. Offline monitoring in extract, raffinate, and dessorbent streams using HPLC systems was carried out to confirm the online data. Samples exiting column 8 along eight consecutive switches were collected to construct the internal concentration profile.

RESULTS AND DISCUSSION

The separation performance of an SMB unit is strongly dependent on the packing characteristics used in the separation system. For heterogeneous columns, the periodic upward movements of the inlet and outlet streams cause changes in the separation performance for each section during a cycle. Table 4 indicates the average porosities for each section during

Table 3. Adsorption parameters of the Langmuir model for ketamine in MCTA

Adsorption parameters	*S*	*R*
q_m	14 ± 1	65 ± 10
b	0.20 ± 0.02	0.11 ± 0.03

Table 4. Average porosity per section in switches 1 to 8

	Switch 1	Switch 2	Switch 3	Switch 4	Switch 5	Switch 6	Switch 7	Switch 8
Section 1	0.64	0.65	0.68	0.69	0.68	0.68	0.69	0.67
Section 2	0.68	0.69	0.68	0.68	0.69	0.67	0.64	0.65
Section 3	0.68	0.68	0.69	0.67	0.64	0.65	0.68	0.69
Section 4	0.69	0.67	0.64	0.65	0.68	0.69	0.68	0.68

each switch. These values were calculated according to experimental values of porosity for each individual column shown in Table 2.

Table 4 indicates five different values of porosities (0.64, 0.65, 0.67, 0.68, and 0.69). These values showed that for each switch, sections 2 and 3 take on different average porosities (except for the first switch), which are not repeated, in the next switches.

Prediction of Separation Regions – Ideal Model

As shown in Table 2, the packing columns have some differences in porosity and Henry coefficients. This non-uniformity in the set of SMB column characteristics may cause a change in the performance of the unit. Some authors have been studying the effect of non-homogeneity in the performance of SMB.[3,10,11] These authors show that the performance parameters have large oscillations during each cycle thus compromising the separation. The main consequence of the heterogeneity of packing columns, in this work, is the generation of five distinct regions of separation (one for each porosity average of the sections). The intersection area of the five triangles is the separation region for a complete cycle. The effect of feed concentration in the complete separation region is also well known and has been extensively discussed.[8,29,30] The separation region is reduced with the increase of feed concentration due to the non-linearity of adsorption isotherms.

The ideal complete separation region for ketamine on MCTA can be observed in Figure 4. A decrease in the separation region with an increase in the total feed concentration was observed. The changes of the average porosity for each section also caused a decrease in the complete separation region. This behavior was more pronounced at the high feed concentrations.

The experimental operating points indicated in Figure 4 were chosen according to Table 5. These conditions were selected in order to obtain *S*-ketamine with high purity in the raffinate stream. In all cases, the operating points (r_2, r_3) do not represent the point of maximum productivity

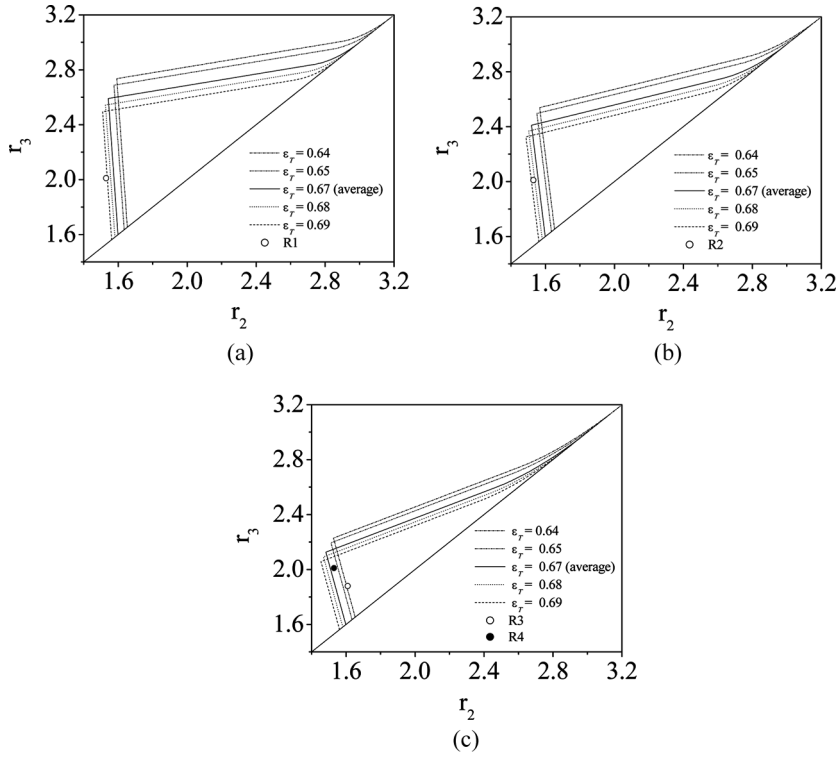

Figure 4. Separation regions based on the equilibrium theory for different feed concentrations and average porosities for each section: (a) Separation region for 1.5 g/L, (b) separation region for 2.5 g/L and (c) separation region for 5 g/L. The experimental points are indicated as reported in Tables 4 and 5.

predicted by the ideal model. These operating points were selected with the purpose of preventing that those occasional fluctuations of the outlet flow rates do not lead to the contamination of the raffinate stream.

Table 5. Operating conditions of the experimental run in SMB unity for ketamine enantiomers separation

			Flow-rate (mL/min)								
Run	c_F (g/L)	t^* (min)	Q_I	Q_{IV}	Q_R	Q_X	Q_F	r_1	r_2	r_3	r_4
R1	1.5	25	1.10	0.38	0.43	0.47	0.18	2.79	1.53	2.01	0.86
R2	2.5	25	1.10	0.38	0.43	0.47	0.18	2.79	1.53	2.01	0.86
R3	5.0	25	1.10	0.37	0.39	0.44	0.10	2.79	1.61	1.88	0.83
R4	5.0	25	1.10	0.38	0.43	0.47	0.18	2.79	1.53	2.01	0.86

SMB Experiments and Non-ideal Simulations

The purity for each experimental condition was calculated by the TMB approach taking into account the non-linearity of isotherms and the non-ideal effects. The axial dispersion is described by $D_L = 0.1\,u$, and overall mass transfer coefficient value (k_m) is $0.75\,min^{-1}$. These parameters were estimated in this work by the inverse method (data not shown).

Figure 5 shows the experimental and simulated results of the internal profile in the steady state for conditions R2 and R3 (see Table 5). The

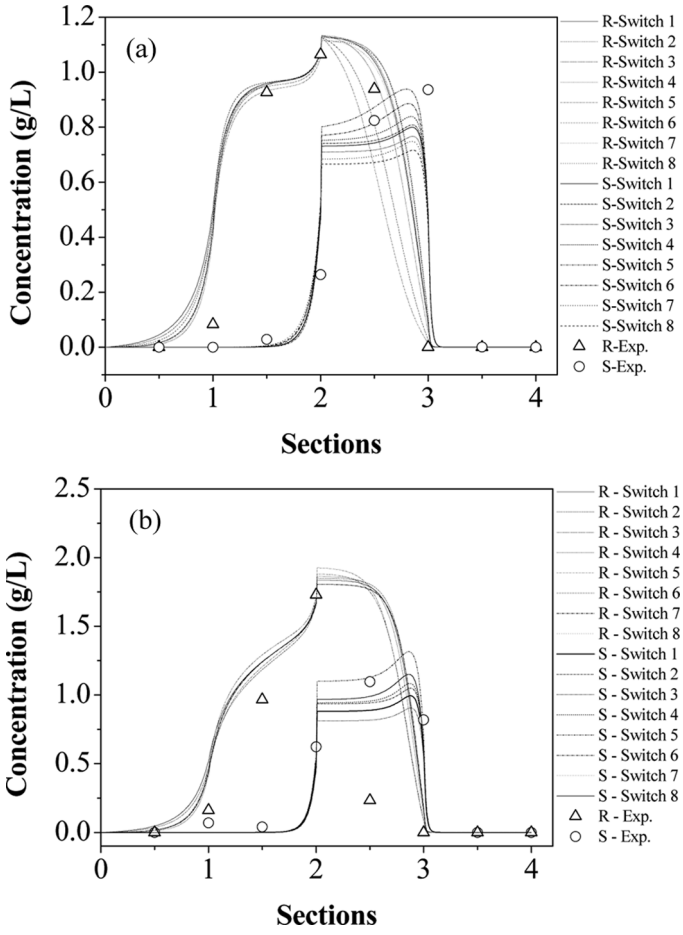

Figure 5. Experimental and simulated internal concentration profiles: (a) Experimental run 2 and (b) Experimental run 3. The symbols (△) indicate the extract and (□) raffinate streams.

experimental profile was obtained by the collection and analysis of samples by HPLC in the outlet of column 8 along eight consecutive switches. The evolution of the concentration along the bed at the end of the last cycle was compared to values obtained mathematically by the TMB approach considering the average porosities (reported in Table 3) and non-ideal effects. The experimental and calculated values of purity are shown in Table 6.

The results show relatively good agreement among the experimental and simulated results (Figure 5). The differences in the experimental and simulated data can be attributed to experimental and mathematical model errors. Experimental errors were provided by small fluctuations of the operating variables, e.g., small flow rate fluctuations in the outlet streams during the switches. Mathematical model errors were provided mainly by high sensitivity to the equilibrium parametric and their uncertainties.

The R1 experimental run achieved high purity level for both raffinate and extract streams and thus confirm the prediction purities with ideal and non-ideal models. However, the extract stream for the R2 experimental run shows a decrease in the purity ($P_X = 98\%$ of the R-ketamine) in disagreement with the TMB ideal model. These results are in agreement with that predicted by the TMB non-ideal model and it is attributed, obviously, to the reduction of the separation region due to the mass transfer resistances. For condition R3, experimental and predicted purity values with the TMB non-ideal model, lead to the conclusion that the operating point R3 is inside the pure raffinate region. However, for condition R4, the operating point was chosen near the triangle vertex

Table 6. Purity stream values reached by model predictions and experimental runs

	R1		R2		R3		R4	
Switches	P_X (%)	P_R (%)	P_X (%)	P_R (%)	P_X (%)	P_R (%)	P_X (%)	P_R (%)
1	99.2	99.9	92.7	100.0	87.8	100.0	96.0	75.7
2	99.2	99.9	94.0	100.0	87.6	100.0	94.3	72.5
3	98.7	99.9	87.2	100.0	84.6	100.0	92.4	72.9
4	99.8	99.9	97.2	100.0	92.0	100.0	91.0	70.8
5	99.9	99.9	99.9	100.0	99.1	100.0	89.5	70.2
6	99.9	99.8	99.8	100.0	97.4	100.0	89.3	68.4
7	99.5	99.4	90.8	100.0	98.0	100.0	87.0	65.2
8	98.0	99.6	84.9	100.0	98.5	100.0	86.0	66.0
Average	99.3	99.8	93.3	100.0	93.1	100.0	90.7	70.2
Experimental	>99.5	>99.5	98.0	>99.5	96.0	99.0	95.0	70.0
SD (%)	0.2	0.3	4.8	0.5	3.0	1.0	4.5	0.3

according to the ideal model (maximum productivity), but inside the pure raffinate region. The predicted results using the TMB non-linear model show that the operating point is found outside of the complete separation region (extract streams enriched). The R4 experimental run data confirms this result. Its purity values were 70% *S*-ketamine for the raffinate stream and 95% *R*-ketamine for the extract stream (see Table 6).

This last observation shows quantitatively that the purity of *S*-ketamine can be decreased due to the influence of resistance to the mass transfer. In this specific case, the operating point is located at the r_2 and r_3 plane in the raffinate pure region, according to the TMB ideal model. However, according to the TMB non-ideal model, it is positioned in the extract enriched region. From an operating condition optimization point of view, this knowledge is fundamental to maintain the performance of the separation process in the specified performance level, e.g., the main constraint for the coupling success of the SMB, and fractional crystallization for *S*-ketamine purification is to ensure an enantiomer excess of 75% of this enantiomer at the outlet of the chromatographic unit.[21]

In general, the experimental runs in the SMB unit show good separation of ketamine enantiomers with high levels of purity in both extract and raffinate streams, but more detailed studies of the operating condition optimization should be developed so as to prioritize S-Ketamine separation with high performance using hybrid process. We can conclude that the TMB non ideal approach, taking into account non-homogenous columns, provides an accurate prediction of the SMB performance for *S*-ketamine separation.

CONCLUSIONS

In this work, the theoretical behavior of SMB units was analyzed by the TMB approach taking into account the non-linearity of adsorption isotherms, non-ideal effects, and non-homogeneity of packing columns. The predicted results were validating with experimental runs. The experimental operating points were selected aiming at the higher purity of the *S*-enantiomer in the raffinate stream. The experimental results obtained with the SMB laboratory unit showed purities above 99.5% for *S*-ketamine in the raffinate stream and above 97.7% for *R*-ketamine in the extract stream. Good agreement between experimental and theoretical results shows that the TMB approach takes into account the non-homogeneity of packing columns, and that mass transfer resistance is an important tool to predict SMB performance.

The results obtained show that this approach can be applied for adequate representation of the SMB behavior, and could contribute to the optimization of the performance for an SMB separation unit aiming

at the resolution of ketamine racemic mixtures and to study the possibility of introducing a hybrid process consisting of continuous chromatography and crystallization to acquire high purity enantiomers with high productivity.

ACKNOWLEDGMENTS

The authors are grateful to Finep (Proc. No. 77.97.0503.00), CNPq (Proc. No. 465707/200-9) and FAPESP (Processes 2001/13168-0 and 2006/02511-9) for financial support and to CRISTÁLIA pharmaceutical company, for kindly providing the racemic anesthetic ketamine and its standard pure enantiomers.

REFERENCES

1. Migliorini, C.; Mazzotti, M.; Zenoni, G.; Morbidelli, M. Simulated moving-bed units with extra-column dead volume. AIChE J. **1999**, *45*, 1411–1421.
2. Francotte, E.; Richert, P.; Mazzotti, M.; Morbidellim, M. Simulated moving bed chromatographic resolution of a chiral antitussive. J. Chromatogr. A. **1998**, *796*, 239–248.
3. Bae, Y.-S.; Moon, J.-H.; Lee, C.-H. Effects of feed concentration of the startup and performance behaviors of simulated moving bed chromatography. Ind. Eng. Chem. Res. **2006**, *45*, 777–790.
4. Silva Jr., I.J.; Veredas, V.; Santos, M.A.G.; Santana, C.C.; Carpes, M.J.S.; Correia, C.R.D. Simulated moving bed chromatography in the wide scale production of enantiomerically pure compounds. Quím. Nova. **2006**, *29*, 1027–1037.
5. Veredas, V.; Carpes, M.J.S.; Correia, C.R.D.; Santana, C.C. Continuous chromatographic separation of a baclofen precursor (*N*-Boc-4-[*p*-chlorophenyl]-2-pyrolidone) in a simulated moving bed using a polyssaccharide carbamate as chiral stationary phase. J. Chromatogr. A. **2006**, *1119*, 156–162.
6. Juza, M.; Mazzotti, M.; Morbidelli, M. Simulated moving bed and its application to chiral technology. Trends in Biotechnol. **2000**, *18*, 108–118.
7. Santos, M.A.G.; Veredas, V.; Silva Junior, I. J.; Correia, C.R.D.; Furlan, L. T.; Santana, C.C. Simulated moving-bed adsorption for separation of racemic mixtures, Braz. J. of Chem. Eng. **2004**, *21*, 127–136.
8. Yu, H.W.; Ching, C.-B. Modeling, simulation and operation performance of a simulated moving bed for enantioseparation of fluoxetine on new β-cyclodextrin columns. Adsorption. **2003**, *9*, 213–223.
9. Stanley, B.J.; Foster, C.R.; Guiochon, G. On the rproducibility of column performance in liquid chromatography and the role of the packing density. J. Chromatogr. A. **1997**, *761*, 41–51.
10. Mihlbachler, K.; Fricke, J.; Yun, T., Seidel-Morgenstern, A.; Schmidt-Traub, H.; Guiochon, G. Effect of the homogeneity of the column set on the performance of a simulated moving bed unity: I. theory. J. Chromatogr. A. **2001**, *908*, 49–70.

11. Mihlbachler, K.; Kaczmarski, K.; Seidel-Morgenstern, A.; Guiochon, G. Measurement and modeling of the equilibrium behavior of the trögeŕs base enantiomers on an amylose-based chiral stationary phase. J. Chromatogr. A. **2002**, *955*, 35–52.
12. Milhlbachler, K.; Seidel-Morgenstern, A.; Guiochon, G. Detailed study of tröger's base separation by SMB. Process AIChE J. **2004**, *50*, 611–624.
13. Yanagihara, Y.; Ohtani, M.; Kariya, S.; Uchino, K.; Aoyama, T.; Yamamura, Y.; Iga, T. Stereoselective high-performance liquid chromatographic determination of ketamine and its active metabolic, norketamine, in humam plasm. J. Chromatogr. B. **2000**, *746*, 227–231.
14. Svensson, J.; Gustafsson, L.L. Determination of ketamine and norketamine enantiomers in plasma by solid-phase extraction and high-performance liquid chromatography. J. Chromatogr. B. **1996**, *678*, 373–376.
15. Nishizawa, N.; Nakao, S.; Nagata, A.; Hirose, T.; Masuzawa, M.; Shingu, K. The effect of ketamine isomers on both mice behavioral responses and c-fos expression in the posterior cingulate and retrosplenial córtices. Brain Res. **2000**, *857*, 188–192.
16. Steiner, K.; Gangkofner, S.; Gruenwald, J-M. Racemic Separation of Ketamine. US2000/6040479, March, 21, 2000.
17. Russo, V.F.T; Russo, E.M.S. Process of Obtainment of Racemic Ketamine Enantiomers: Process of Obtainment of Pharmaceutically Acceptable Salts from Racemic Ketamine Enantiomers and Use of Pharmaceutically Acceptable Salts Obtained by Means of Said Mentioned Process. US2003/0212143 A1, Nov.13, 2003.
18. Wang, X.J.; Wiehler, H.; Ching, C.B. Study of the Characterization and crystallization of 4-hydroxy-2-pyrrolidone. Chirality **2004**, *16*, 220–227.
19. Silva Jr., I.J.; Santos, M.A.G.; Veredas, V.; Santana, C.C. Experimental determination of chromatographic separation parameters of ketamine enantiomers on MCTA. Sep. Purif. Technol. **2005**, *43*, 103–110.
20. Silva Jr., I.J.; Santos, M.A.G.; Veredas, V.; Santana, C.C. Effect of temperature on chiral separation of ketamine enantiomers by high-performance liquid chromatography. Sep. Sci. Technol. **2005**, *40*, 2593–2611.
21. Barros, G.O.F.; Tamagawa, R.E.; Santana, C.C.; Miranda, E.A. Ternary Phase Diagram of Ketamine ((R/S)-2-(2-chlorophenyl)2-methylamine cyclohexanone) in Ethanol and Preliminary Studies Aiming to the Fractional Crystallization of S-ketamine, submitted for publication, 2007.
22. Azevedo, D.C.S. Separation/reaction in Simulated Moving Bed: Application to the Production of Industrial Sugars. PhD Thesis, Universidade do Porto, Porto, Portugal, 2001.
23. Azevedo, D.C.S.; Rodrigues, A.E. Design of a simulated moving bed in the presence of mass-transfer resistances. AIChE J. 1999, *45*, 956–966.
24. Minceva, M.; Rodrigues, A.L. Two-level optimization of an existing SMB for *p*-xylene separation. Comp. Chem. Eng. **2005**, *29*, 2215–2228.
25. Barreto Jr, A.G. Design of Chromatographic Systems to Lapachol Separation, PhD Thesis, COPPE/UFRJ, Rio de Janeiro/RJ/Brasil, 2005, Available in Portuguese.

26. Maliska, C.L. Transferência de Calor e Mecânica dos Fluidos Computacional, 2ª Edição, LTC Editora, São Paulo, Brasil, **2004**, Available in Portuguese.
27. IMSL, Fortran subroutine for mathematical applications, Visual Numerics, Inc., **1997**.
28. Zenoni, G.; Pedeferri, M.; Mazzotti, M.; Morbidelli, M. On-line monitoring of enantiomer concentration in chiral simulated moving bed chromatography. J. Chromatogr. A. **2000**, *888*, 73–83.
29. Mazzotti, M.; Storti, G.; Morbidelli, M. Optimal operation of simulated moving bed units for nonlinear chromatographic separations. J. Chromatogr. A. **1997**, *769*, 3–24.
30. Migliorini, C.; Mazzotti, M.; Zenoni, G.; Morbidelli, M. Continuous chromatographic separation through simulated moving beds under linear and nonlinear conditions. J. Chromatogr. A. **1998**, *827*, 161–173.

Received March 1, 2008
Accepted May 19, 2008
Manuscript 6317